

## Bistability and hysteresis of solitons in inhomogeneously doped fibers with saturating nonlinearity

Ajit Kumar

*Department of Physics, Indian Institute of Technology, Hauz Khas, New Delhi 110016, India*

(Received 5 June 1997; revised manuscript received 8 May 1998)

Inhomogeneous doping of a silica glass fiber is proposed to have bistable soliton propagation. The properties of the solitons in one of the possible models are studied and interpreted. [S1063-651X(98)05409-9]

PACS number(s): 42.81.-i, 42.65.Tg

Ever since the pioneering work of Kaplan [1,2] there has been a constant endeavor from researchers to obtain a suitable and practically feasible model for bistable soliton propagation in doped fibers that show nonlinear saturation in the intensity dependent refractive index [3–10]. Initial studies of Gatz and Herrmann [3,4], Sombra [5], and Kumar, Kurz, and Lauterborn [6–8] showed that fibers made of semiconductor-doped glasses support two-state solitons that represent pulses with the same pulsewidth but with different energies or powers. This property is similar to the property of a bistable system in the sense that for a given input control parameter (pulsewidth) there are two output states of the system. However, this is a different kind of bistability compared to the original one envisioned by Kaplan [1]. Because of this researchers started studying pulse propagation in doubly doped fibers. Here also, as shown by Gatz and Herrmann [4], one can have only two-state solitons. Later, Enns and Edmundson [9] showed that Kaplan-type bistable solitons can exist if one could have a fiber made of doped glass with three dopants. This fact has been confirmed by Kumar *et al.* [10] in a modified model. The advantage of having bistable solitons lies in the fact that with them one would be able to construct ultrafast all-optical switches besides being able to perform several other useful operations (for example, fission of solitons, fusion of solitons, radiation stripping, etc. [11]) in a multipoint nonlinear directional coupler configuration.

In the given paper we propose a mechanism that would enable us to have bistable solitons in a fiber made of doped glass with two dopants provided the second dopant is inhomogeneously distributed over a restricted region of the cross section of the fiber core. As it turns out, in such a system, one can have bistable solitons and the system is also capable of showing hysteretic behavior as predicted by Kaplan.

Consider a monomode isotropic doped glass fiber with circular cross section. Let the glass be doped with two dopants. One of the dopants is assumed to be homogeneously distributed over the entire fiber core while the second has inhomogeneous radial distribution over the cross section enclosed between  $0 \leq r \leq a$ . Also the second dopant is supposed to be defocusing. The inhomogeneous distribution is such that the concentration of the second dopant is minimum on the fiber axis and increases exponentially away from it up to  $r = a$ . The concrete value of  $a$  will be determined later. With these things in mind we proceed to model nonlinear pulse propagation in such a fiber.

Let  $z$  be the direction along the fiber. The nonlinear wave

equation in the core region of the fiber can be written as

$$\vec{\nabla}^2 \vec{E} - \frac{1}{c^2} \frac{\partial^2 \vec{D}^L}{\partial t^2} = \frac{1}{c^2} \frac{\partial^2 \vec{D}^{NL}}{\partial t^2}, \quad (1)$$

where  $\vec{D}^L$  and  $\vec{D}^{NL}$  are the linear and the nonlinear parts, respectively, of the electric induction vector  $\vec{D}$ .  $\vec{D}^L$  is given by

$$\vec{D}^L = \int_0^\infty \varepsilon(t') \vec{E}(t-t') dt', \quad (2)$$

where  $\varepsilon$  is the linear permittivity of the fiber.

Because of inhomogeneous doping the nonlinear dielectric constant will acquire a radial dependence in the region  $0 \leq r \leq a$ . Therefore, the nonlinear part of  $\vec{D}$  is taken to be

$$\vec{D}^{NL} = [\varepsilon_2^{(1)} + \alpha \varepsilon_2^{(2)} f(r)] \frac{|\vec{E}|^2 \vec{E}}{1 + |\vec{E}|^2 / I_s}, \quad (3)$$

where  $\varepsilon_2^{(j)}$ ,  $j = 1, 2$  are the Kerr coefficients for the nonlinear permittivity of the first ( $j = 1$ ) and second dopant ( $j = 2$ ), respectively,  $I_s$  is the saturation intensity, which, for simplicity, is taken to be the same for both dopants,  $f(r)$  stands for the radial dependence of the nonlinear permittivity, and  $\alpha$  stands for the second dopant concentration relative to the first dopant concentration. Note that  $\varepsilon_2^{(j)}$ ,  $j = 1, 2$  is related to the Kerr coefficient  $n_2^{(j)}$ , for the nonlinear refractive index change, through the relation [7]  $\varepsilon_2^{(j)} = 2n_0 n_2^{(j)}$ ,  $j = 1, 2$ ;  $n_0$  being the linear refractive index of the fiber core. Before moving further we have to take a concrete form of the function  $f(r)$ . We take it as follows:

$$f(r) = \begin{cases} \exp(\chi r^2) & \text{for } r < a \\ 0 & \text{for } r \geq a, \end{cases} \quad (4)$$

where  $\chi$  is a constant. Now, as usual [7], we represent the electric field envelope amplitude in the following form

$$\vec{E}(x, y, z, t) = \vec{e} R(\vec{r}) A(z, t) \exp[-i(\omega t - \beta_0 z)], \quad (5)$$

where  $\vec{e}$  is the unit vector in the direction of polarization,  $\beta_0$  is the propagation constant,  $R(\vec{r})$  is the mode function giving the transverse distribution of the field in the mode, and  $A(z, t)$  is the complex envelope amplitude of the pulse. Fur-

ther, adopting the customary slowly varying envelope approximation and performing the averaging over the fiber cross section by taking the first moment of the differential equation with respect to the modal field distribution (which, as usual, is assumed to be Gaussian,  $R(\vec{r}) = \exp(-r^2/2r_0^2)$  we obtain, from Eqs. (1)–(5), the following dimensionless evolution equation for the normalized complex envelope amplitude  $q(\xi, \tau)$  for the case  $\chi r_0^2 = 2$ :

$$iq_\xi + \frac{1}{2}q_{\tau\tau} + f(|q|^2)q = 0, \quad (6)$$

where

$$\begin{aligned} f(|q|^2) = & 1 - \frac{\ln(1+|q|^2)}{|q|^2} \\ & - \alpha\delta\{\sigma|q|^2 + |q|^2\ln[1 + \exp(-\sigma)|q|^2] \\ & - |q|^2\ln(1+|q|^2)\}. \end{aligned} \quad (7)$$

The dimensionless variables in Eqs. (6) and (7) are given by

$$\begin{aligned} q &= A/\sqrt{I_s}, \xi = (\omega n_2^{(1)} I_s / c)z, \\ \tau &= \sqrt{[\omega n_2^{(1)} I_s / c(-k_{\omega\omega})]} \left( t - \frac{z}{v_g} \right), \end{aligned} \quad (8)$$

$$\delta = |n_2^{(2)}|/n_2^{(1)}, \quad (9)$$

and

$$\sigma = \frac{a^2}{r_0^2}. \quad (10)$$

Here  $r_0$  is the radial distance from the fiber axis at which the field intensity drops by a factor  $1/e$ . Also, in deriving this equation we have taken into account that  $n_2^{(2)} < 0$  for the defocusing second dopant. Note that  $\chi r_0^2 = 2$  has been chosen for the simplicity of the model equation rather than anything else. In general, one can take any sensible value of  $\chi r_0^2$  and obtain the model equation.

### THE SOLITON SOLUTION

We look for the fundamental soliton solutions of Eq. (6) in the following form:

$$q(\xi, \tau) = \sqrt{\Psi(\tau)} \exp(i\beta\xi), \quad (11)$$

where

$$\lim_{|\tau| \rightarrow \infty} \Psi(\tau) = \lim_{|\tau| \rightarrow \infty} [d\Psi(\tau)/d\tau] = 0, \quad (12)$$

where  $\beta$  has the meaning of the nonlinear propagation constant shift. Using this form of the soliton solution we obtain from Eqs. (6), (7), and (10) the following ordinary differential equation for  $\Psi(\tau)$ :

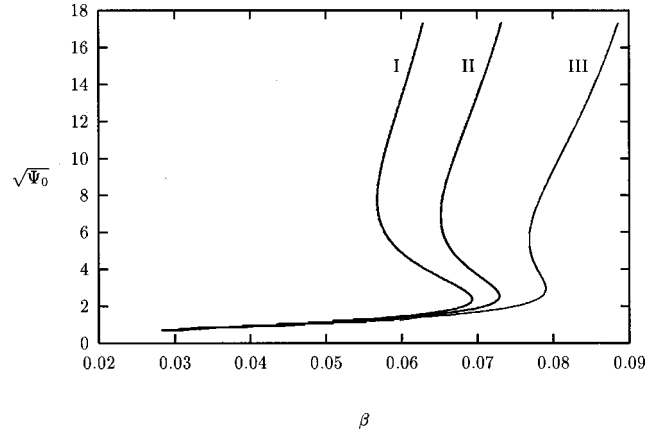


FIG. 1. Soliton peak amplitude  $\sqrt{\Psi_0}$  vs nonlinear propagation constant  $\beta$  for  $\alpha=0.04$ ,  $\delta=5$ , and three values of  $\sigma$  [1.7: (curve III), 1.715 (curve II), and 1.725 (curve I)].

$$\begin{aligned} \frac{\Psi''}{4\Psi} - \frac{(\Psi')^2}{8\Psi^2} + (1-\beta) - \frac{\ln(1+\Psi)}{\Psi} \\ - \alpha\delta\sigma\Psi + \alpha\delta\Psi \ln(1+\Psi) \\ - \alpha\delta\Psi \ln[1 + \exp(-\sigma)\Psi] = 0. \end{aligned} \quad (13)$$

Here the prime stands for the ordinary derivative with respect to  $\tau$ .

### NUMERICAL RESULTS AND DISCUSSIONS

For a given set of the parameters  $\alpha$ ,  $\delta$ , and  $\sigma$  and a given initial amplitude  $\sqrt{\Psi_0}$  we first determine the appropriate value of the nonlinear propagation constant  $\beta$  by exploiting the first integral of Eq. (13), the boundary conditions given by Eq. (12), and the fact that we are looking for the bright soliton solutions with a maximum at  $\tau=0$ . This yields

$$\begin{aligned} \beta = & 1 - \frac{\alpha\delta\sigma}{2} \Psi_0 - \frac{\alpha\delta}{2} \left( \frac{e^\sigma - 1}{2} \right) \\ & - \frac{\alpha\delta}{2} \left( \Psi_0 - \frac{e^{2\sigma}}{\Psi_0} \right) \ln(1 + \Psi_0) \\ & + \frac{\alpha\delta}{2} \left( \Psi_0 - \frac{1}{\Psi_0} \right) \ln(1 + \Psi_0) - \frac{F_1(\Psi_0)}{\Psi_0} \end{aligned} \quad (14)$$

where

$$F_1(\psi_0) = \int_0^{\psi_0} \frac{\ln(1+y)}{y} dy. \quad (15)$$

We then use this value of  $\beta$  to determine the soliton shape by numerically integrating Eq. (13) via the Runge-Kutta method. Finally, we numerically compute the soliton energy  $P$  according to the formula

$$P = \int_{-\infty}^{\infty} |q|^2 d\tau. \quad (16)$$

The results are shown in Figs. 1–4. In Fig. 1 we have plotted  $\sqrt{\Psi_0}$  as a function of the nonlinear addition to the

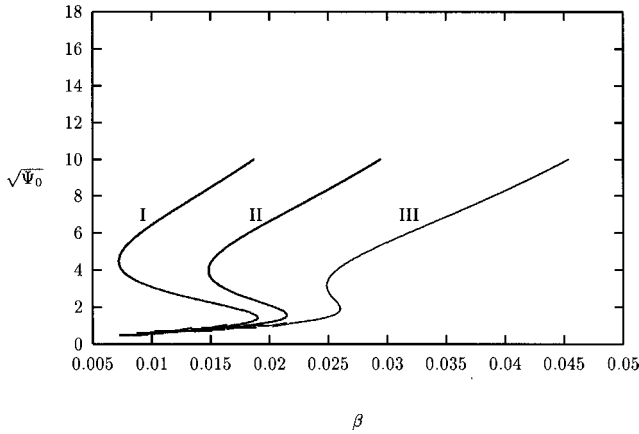


FIG. 2. Soliton peak amplitude  $\sqrt{\Psi_0}$  vs nonlinear propagation constant  $\beta$  for  $\alpha=0.04$ ,  $\delta=7.5$ , and three values of  $\sigma$  [ $1.4$  (curve III),  $=1.415$  (curve II), and  $=1.425$  (curve I)].

propagation constant  $\beta$ . All the plots in this figure correspond to  $\alpha=0.04$  and  $\delta=5$  but different values of  $\sigma$ :  $1.7$  (curve III),  $1.715$  (curve II), and  $1.725$  (curve I). In Fig. 2 we have the same plots for  $\alpha=0.04$ ,  $\delta=7.5$ , and  $\sigma=1.4$  (curve III),  $\sigma=1.415$  (curve II), and  $\sigma=1.425$  (curve I). It is quite clear from these figures that the nonlinear addition to the propagation constant  $\beta$  is a multivalued function of the soliton peak amplitude  $\sqrt{\Psi_0}$ . It is also visible that for given values of  $\alpha$ ,  $\delta$  and the maximum peak amplitude (and hence peak power) the interval of  $\beta$ , for which bistable solitons are possible, depends on  $\sigma$ : the larger the value of  $\sigma$  the larger the  $\beta$  range of bistability.

Figure 3 contains the plot of the soliton energy  $P$  as a function of  $\beta$ . The curve labeled I in Fig. 3 corresponds to  $\alpha=0.04$ ,  $\delta=7.5$ , and  $\sigma=1.4$  while the curve labeled II corresponds to  $\alpha=0.04$  and  $\delta=5$  and  $\sigma=1.7$ . It is clear from Fig. 3 that  $P(\beta)$  is S shaped, and ensures the bistable and hysteretic behavior of the soliton solutions (see pages 1292 and 1293 in Ref. [1]). Further, Fig. 3 shows that for a given value of  $\beta$  there are three values of  $P$  for which soliton solutions exist. Soliton solutions corresponding to the positive slope branches of the  $P(\beta)$  curve satisfy the stability criterion [1,2] given by  $(dP/d\beta) > 0$ , and are stable, while

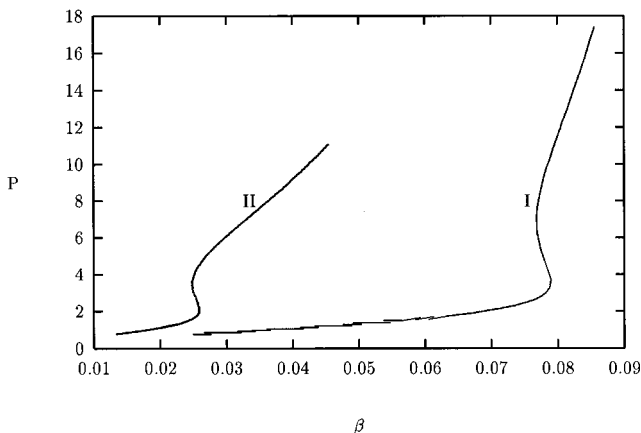


FIG. 3. Soliton energy  $P$  vs nonlinear propagation constant  $\beta$  for  $\alpha=0.04$ ,  $\delta=7.5$ , and  $\sigma=1.4$  (curve II) and  $\alpha=0.04$ ,  $\delta=5$ , and  $\sigma=1.7$  (curve I).

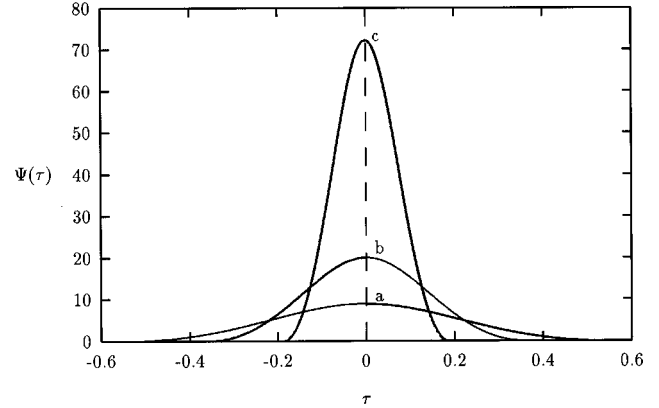


FIG. 4. The soliton shape  $\Psi(\tau)$  for  $\alpha=0.04$ ,  $\delta=5$ , and  $\sigma=1.7$ , corresponding to the  $P(\beta)$  curve of Fig. 3 (curve III). The smallest soliton (curve  $a$  with  $P=3.665$ ) belongs to the lower positive slope branch of the  $P(\beta)$  curve, while the tallest soliton (curve  $c$  with  $P=10.562$ ) belongs to the upper positive slope branch of the  $P(\beta)$  curve. These soliton solutions are stable. The soliton solution, curve  $b$ , with  $(P=5.49)$  belongs to the negative slope branch of the  $P(\beta)$  curve and is unstable.

those corresponding to the negative slope branch are unstable.

Before proceeding further we would like to note here that we have studied soliton solutions in the given model for a wide range of the parameters  $\alpha$  and  $\delta$ . We find that for each pair of values of the parameters  $\alpha$  and  $\delta$  the soliton solutions exist for any value of the parameter  $\sigma$ . However, bistability exists only for  $\sigma$  greater than a particular value  $\sigma_{th}$ , which is different for different pairs.

For illustration, we have depicted the soliton shapes in Fig. 4 corresponding to all three branches of the  $P(\beta)$  curve. Here  $\alpha=0.04$  and  $\delta=5$  and  $\sigma=1.7$ . All these solutions have the same value of  $\beta=0.079\ 002\ 75$ . The smallest soliton in Fig. 4 (curve  $a$  with energy  $P=3.665$ ) belongs to the lower positive slope branch of the  $P(\beta)$  curve and is stable while the tallest soliton in Fig. 4 (curve  $c$  with energy  $P=10.562$ ) belongs to the upper positive slope branch of the  $P(\beta)$  curve and is also stable. The soliton solution given by curve  $b$  with energy  $P=5.49$  belongs to the negative slope branch of the  $P(\beta)$  curve and is unstable. The pair of values of  $\alpha$  and  $\delta$ , for which the results have been presented here, is just a representative pair.

In order to have a feeling of the orders of magnitudes of the soliton characteristics, let us consider the case of a fiber made of silica glass homogeneously doped with PTS and inhomogeneously doped with CdS and Se ( $\text{CdS}_x\text{Se}_{1-x}$ ) such that  $\alpha=0.04$ . The experimental value of  $n_2$  for PTS, in the resonant case, is  $2 \times 10^{-11} \text{ cm}^2/\text{W}$  and for  $\text{CdS}_x\text{Se}_{1-x}$  it is  $-10^{-10} \text{ cm}^2/\text{W}$  [13]. Hence for these dopants  $\delta=5$  and the case corresponds to one of the sets of parameters used in the given work. If we take  $\lambda=1.55 \mu\text{m}$ ,  $n_0=1.44$ ,  $I_s=200 \text{ MW}/\text{cm}^2$ , and  $k_{\omega\omega}=27(\text{ps}^2/\text{K m})$  and insert them into the rescaling relation given by Eq. (8) we obtain that  $\tau=1$  corresponds to  $411 \text{ fs}$ . For this case the upper positive slope branch soliton of Fig. 4 has a full width at half maximum (FWHM) equal to  $123 \text{ fs}$  and a peak intensity of  $144.40$

$\times 10^7$  W/cm<sup>2</sup> and the lower positive slope branch soliton has a FWHM of 205 fs and a peak intensity of  $19.60 \times 10^7$  W/cm<sup>2</sup>.

Further analysis shows that if, for a given set of values of  $\alpha$  and  $\delta$ , we go on increasing the value of  $\sigma$  (i.e., go on increasing the region of inhomogeneous doping with the second defocusing dopant) then there appears an interval of  $\sqrt{\Psi_0}$  for which  $\beta$  becomes negative and beyond this interval returns to take on positive values. For these values of the initial soliton amplitudes for which  $\beta$  is negative we obtain cnoidal wave solutions and not the soliton solutions. Hence for these values of  $\sigma$  the lower and the upper positive slope branch solitons are separated by cnoidal solutions and hence, in the terminology of Snyder *et al.* [12], these bistable solitons are discontinuous solitons.

### CONCLUSIONS

We report the results of our studies related to bistable solitons in doped fibers. The work is based on the idea of an

inhomogeneously doped fiber. To the best of our knowledge such a system has not been considered and studied so far. We have obtained and studied the properties of these solitons in one of the possible models. Our analysis shows that for a given set of the parameters  $\alpha$ ,  $\delta$ , and  $\sigma$  there exist three soliton solutions that represent light pulses with different energies and shapes but with the same nonlinear propagation constant  $\beta$ . Two stable branches of solitons are separated by an unstable branch as required for switching from one bistable state to the other [9]. We believe that with the available advanced technology for doping materials in a controlled manner it should be possible to have fibers with the properties described here and hence our results should be useful for practical applications.

The given work is partially supported by the Department of Science and Technology, Government of India, through a research project grant.

- 
- [1] A. E. Kaplan, Phys. Rev. Lett. **55**, 1291 (1985).
  - [2] A. E. Kaplan, IEEE J. Quantum Electron. **21**, 1538 (1985).
  - [3] S. Gatz and J. Herrmann, J. Opt. Soc. Am. B **8**, 2296 (1991).
  - [4] S. Gatz and J. Herrmann, Opt. Lett. **17**, 484 (1992).
  - [5] A. S. B. Sombra, Opt. Commun. **94**, 92 (1992).
  - [6] Ajit Kumar and Atul Kumar, Opt. Commun. **125**, 377 (1996).
  - [7] Ajit Kumar, T. Kurz, and W. Lauterborn, Phys. Rev. E **53**, 1166 (1996).
  - [8] Ajit Kumar, Atul Kumar, T. Kurz, and W. Lauterborn, Pure Appl. Opt. **5**, 283 (1996).
  - [9] R. H. Enns and D. E. Edmundson, Phys. Rev. A **47**, 4524 (1993).
  - [10] Ajit Kumar, T. Kurz, and W. Lauterborn, Phys. Lett. A **235**, 367 (1997).
  - [11] R. H. Enns, R. Fung, and S. S. Rangnekar, IEEE J. Quantum Electron. **27**, 252 (1991).
  - [12] A. W. Snyder, D. J. Mitchell, and Y. S. Kivshar, Mod. Phys. Lett. B **9**, 1479 (1995).
  - [13] G. I. Stegeman and R. H. Stolen, J. Opt. Soc. Am. B **6**, 652 (1989).